Numerical Methods in Civil Engineering, 6-1 (2021) 50-62

Numerical Methods in Civil Engineering

Journal Homepage: https://nmce.kntu.ac.ir/

An analytical solution for stability analysis of unrestrained tapered thin-walled FML profile

Masoumeh Soltani[*] and Azadeh Soltani[**]

ARTICLE INFO

RESEARCH PAPER

Article history:
Received:
April 2021.
Revised:
July 2021.
Accepted:
August 2021.

Keywords:
Fiber-metal laminates; I-section; Tapered beam; Lateral-torsional stability; Classical lamination theory; Galerkin's method

Abstract:

The main purpose of this study is to compare the lateral buckling behavior of laterally unrestrained Fiber-Metal Laminate (FML) and composite thin-walled beam with varying cross-section under transverse loading. It is supposed that all section walls (the web and both flanges) are composed of two metal layers at the outer sides of the fiber-reinforced polymer laminates. The classical lamination theory and Vlasov's model for thin-walled cross-section have been adopted to derive the coupled governing differential equations for the lateral deflection and twist angle. Employing an auxiliary function, the two governing equations are reduced to a single fourth-order differential equation in terms of twist angle. To estimate the lateral buckling load, Galerkin's method is then applied to the resulting torsion equilibrium equation. Eventually, the lateral stability resistance of FML and laminated composite web-tapered I-beam under uniformly distributed load has been compared to each other considering the effects of some significant parameters such as laminate stacking sequence, metal volume fraction, transverse load position, and web tapering ratio. The results show that increasing the metal volume fraction leads to enhance the linear buckling strength of glass-reinforced aluminum laminate I-beam under transverse loading. For the optimum lamination, it is seen that the lateral buckling load increases approximately 25% by raising the metal volume percentage from 0% to 20%.

1. Introduction

Thin-walled members comprise a wide range of structural elements. The profile of these elements includes connected thin plates encompassing open, closed, or a combination of both. These members are increasingly used in various industries and engineering structures such as civil engineering and aerospace due to their ability to consume materials economically and optimize the weight of the structure. Today, the fabrication of thin-walled beams from various materials such as steel, wood, fiber-reinforced composite materials, and functionally graded materials has become possible by developing pultrusion and assembly methods. Fiber metal laminations (FMLs) are a new class of hybrid materials built from several thin sheets of metal alloys and fiber-reinforced epoxy composite plies. These laminates possess the desirable features of metal such as ductility, damage tolerance, excellent resistance to impact and environmental conditions, and advantages of the reinforced polymeric composites such as good fatigue resistance, durability, and high value of stiffness-to-weight and strength-to-weight ratios. Due to the conspicuous characteristics of FMLs, the use of fiber-metal hybrid composite structures in the design of submarine and aircraft industries has become increasingly common throughout the years. A literature review shows that several investigations have been performed on the behavior of laminated composite components such as thin-walled beams, cylinders, shells, and plates. In the following, a short description of some of these studies is presented.

A new finite element formulation applicable for stability analysis of arbitrary cross-sections of the tapered thin-walled beams was described by Rajasekaran [1]. Nam et al. [2] used a genetic algorithm to optimize the arrangement of metal-fiber multilayer composite shells under different loading cases. They indicated that metal-fiber multilayer shells made of carbon fiber-reinforced polymer laminates are more resistant to random and unforeseen forces in most loading conditions. Based on the

* *Corresponding Author: Assistant Professor, Department of civil engineering, University of Kashan, Kashan, Iran, E-mail: msoltani@kashanu.ac.ir*
** *MSc Student in Structural Engineering, Department of civil engineering, University of Kashan, Kashan, Iran.*

classical lamination theory, Lee et al. [3-6] studied flexural behavior, dynamics, and stability of thin-walled open and closed beam profiles made of symmetrical multilayer fiber composite using finite element method and cubic shape function. Vibration and instability analyses of FGM spinning circular cylindrical thin-walled beams were performed by Oh et al. [7]. Rajasekaran and Nalinaa [8] assessed the vibrational characteristics and buckling behavior of non-prismatic composite spatial members having generic thin-walled sections via the finite element method within the context of the non-linear strain displacement relationship. Magnucka-Blandzi [9] examined the lateral stability limit state of simply supported I-beam under combined loads, including uniformly distributed load, longitudinal force, and gradient moment. With the finite element methodology, the flexural-torsional coupled free vibrational behavior and buckling problem of thin-walled composite beams were precisely investigated by Vo and Lee [10], considering the impacts of axial load on the vibration characteristics. In another study, Moon et al. [11] evaluated the buckling behavior of a medium-thickness carbon-epoxy composite cylinder under external hydrostatic pressure by modeling in Nastran finite element software. To estimate the buckling resistance of simply supported thin-walled structural members made of Fiber Reinforced Polymer (FRP) loaded by axially and uniformly transverse forces, Ascione et al. [12] developed a mechanical model based on the assumptions of small strains and moderate rotations. Further, Arajo et al. [13] dynamically analyzed sandwich sheets using natural materials and piezoelectric composite layers by applying the finite element method. In another study, Ravishankar et al. [14] reported the influence of type fiber-reinforced epoxy composite materials, Metal Volume Fraction (MVF), and angular velocity on the free vibrational response of rotating beams made of FMLs and or functionally graded materials using finite element software. Banat et al. [15-17] evaluated the buckling behavior of FMLs composite thin-walled beams with C- and Z-shaped sections under axial compressive force using ANSYS finite element software. Further, they perused the effect of layer arrangement on the compressive capacity and compared the outcomes of software modeling with laboratory results. In addition, Hallival et al. [18], in a laboratory study, investigated the behavior of fiber-metal multilayers by adding resin under an impact force and reported that adding resin between the layers results in decreasing the separation by 40-50% and increasing the compressive strength by approximately 30%**.** Based on a generalized layered global-local beam (GLGB) theory, Lezgy-Nazargah [19] proposed an efficient finite element model for the elasto-plastic analysis of beams with thin-walled cross-section. Mohandes and Ghasemi [20] employed finite strain theory on free vibration of microlaminated composite Euler-Bernoulli beam in a thermal environment. Mohandes et al. [21] extracted the equations governing the free vibration of the cylindrical shell made of metal-fiber composite layers based on the first-order shear deformation theory. Their work evaluated various parameters such as different material properties of composite fibers, lay-up arrangement, fiber angle, boundary conditions, number of vibrational modes, and metal volume fraction. In another study, Ahmadi and Rasheed [22] employed the generalized semi-analytical technique to analyze the lateral-torsional buckling of anisotropic laminated beams with rectangular thin-walled cross-section subjected to simply supported end supports based on the classical laminated plate theory. Within the context of first-order shear deformation theory and using a semi-analytical solution methodology, the mechanical response of thin-walled laminated beams with constant open and/or closed cross-sections was assessed by Wackerfuß and Kroker [23]. Through a one-dimensional finite element model, Asadi et al. [24] analyzed the linear stability behavior of laminated composite beams with thin-walled open/closed sections under various boundary conditions. In their study, the impacts of transverse shear deformation and out-of-plane warping of the beam section are considered. Within the context of Love's first approximation shell theory, Ghasemi and Mohandes [25] presented a comparative study between the vibrational responses of FML and composite cylindrical shells. Soltani [26] perused the flexural-torsional buckling behavior of the tapered sandwich I-beam with porous core using the differential quadrature method. Additionally, the mechanical responses of composite thin-walled beams with different geometries and subjected to various types of loading cases and end conditions were exhaustively assessed by Lezgy-Nazargah et al. [27-32] using the concept of equivalent layered composite cross-section.

As mentioned earlier, most of the studies conducted on the behavior analysis of fiber/metal laminated composites have focused on cylindrical shells, while few laboratory studies have been performed on the stability characteristics of thin-walled FML beams [15-17]. Due to the application of hybrid fiber-metal composite thin-walled elements in aircraft and spacecraft structures and the blades of wind turbines and helicopters, there is a strong scientific need to precisely assess the lateral stability strength of thin-walled FML profile under transverse loads. Thus, the current research is aimed to probe the lateral-torsional buckling characteristics of FML tapered I-beams according to Vlasov's assumptions [33]. Based on this model and using small displacements theory, the lateral-torsional stability behavior of thin-walled beams with arbitrary laminations is usually governed by three fourth-order differential equations coupled in terms of the lateral and vertical displacements as well as the torsion angle. Perusing the critical state of thin-walled composite members subjected to combined transverse loads and compressive axial force is complicated in the presence of flexural-torsional coupling. This procedure seems to be more problematic in the presence of thin-walled beams with varying web and/or flanges. To investigate the lateral buckling behavior of this type of member, the 12*12 static and buckling stiffness matrices can also be formulated based on twelve displacement parameters, namely: two translations, twist, two rotations, and warping at each end node [3-6, 10]. In the case of doubly-symmetric thin-walled composite beams with symmetric laminations under bending moment about the strong principal axis of the cross-section, a two-noded element with four degrees of freedom at each node

and resultantly 8*8 static element stiffness matrices are commonly required to study the lateral stability behavior [3-6, 10]. Although the finite element technique is capable of estimating the buckling loads with the desired precision, it requires a considerable amount of time to be executed. For this reason, the linear lateral buckling behavior of tapered thin-walled FML beam with doubly-symmetric I-section is analyzed by means of Galerkin's method. The main advantage of this methodology is simplicity, reducing computational effort, and consequently saving computing time. To this end, the following steps are considered:

Using classical laminated theory and energy method, the coupled governing differential lateral-torsional stability equations for the lateral deflection and torsion are extracted by implementing Vlasov's model for thin-walled cross-sections. Following the methodology expanded by Soltani et al. [34-36], the two lateral stability equations are uncoupled and reduced to a single fourth-order differential equation in terms of the twist angle. The resulting formulation can be applied for calculating the lateral-buckling load of laminated composite I-beam under different boundary conditions and loading cases. However, only the simply supported beam with free warping at both supports is considered in this study. The trigonometric function, which satisfies the simply supported beam end conditions, is then used to acquire the analytical solutions with Galerkin's method. To check the accuracy and the efficiency of the proposed methodology, our results are compared with numerical ones from the ANSYS code, and good agreement is observed. By performing a comprehensive parametric example, the outcomes of lateral buckling analysis of simply supported laminated web-tapered I-beam under uniformly distributed load is given in terms of the impacts of some representative parameters such as lay-up arrangement, metal volume fraction, web tapering ratio, and loading position. Finally, the best lay-up of the internal fiber composite layers is introduced by examining different stacking sequences.

2. Formulations

A schematic of thin-walled FML beam with length L varying I-section subjected to uniformly distributed load is shown in Fig. 1. The orthogonal right-hand Cartesian coordinate system (*x, y, z*) is adopted, wherein x denotes the longitudinal axis and y and z are the first and second principal bending axes parallel to the flanges and web, respectively. The origin of these axes (*O*) is located at the centroid of the cross-section. It is supposed that all section walls are composed of two metal layers at the outer sides of the fiber-reinforced polymer laminates. Based on small displacements assumption and Vlasov's thin-walled beam theory for non-uniform torsion, the displacement fields can be expressed as [33]:

$$U(x,y,z) = u_0(x) - y\frac{dv(x)}{dx} - z\frac{dw(x)}{dx} - \omega(y,z)\frac{d\theta(x)}{dx} \quad (1a)$$

$$V(x,y,z) = v(x) - z\,\theta(x) \quad (1b)$$

$$W(x,y,z) = w(x) + y\,\theta(x) \quad (1c)$$

In these equations, U is the axial displacement and displacement components V and W represent lateral and vertical displacements (in direction y and z). The term $\omega(y,z)$ signifies a cross-section variable that is called the warping function, which can be defined based on Saint-Venant's torsion theory and θ is twisting angle.

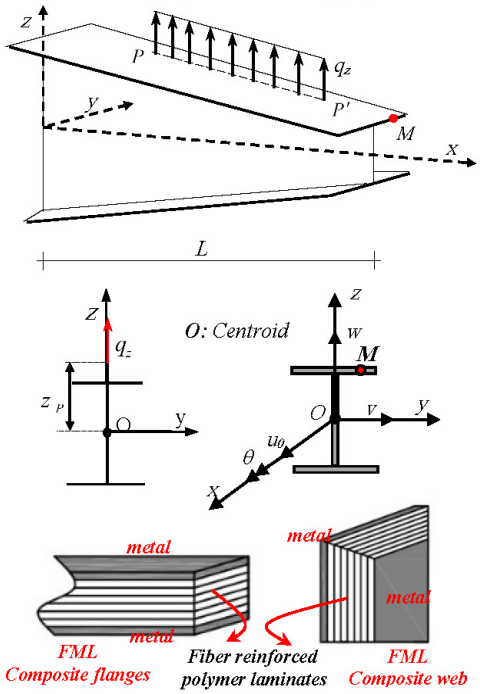

Fig. 1: Beam with variable doubly symmetric I-section under external distributed loads: Coordinate system, notation for displacement parameters, definition of load eccentricities, and web and flanges lay-up arrangement.

The Green's strain tensor components which incorporate the large displacements including linear and non-linear strain parts are given by:

$$\varepsilon_{ij} = \varepsilon_{ij}^{l} + \varepsilon_{ij}^{*} \quad i,j = x,y,z \quad (2a)$$

$$\varepsilon_{ij} = \frac{1}{2}\left(\frac{\partial U_i}{\partial x_j} + \frac{\partial U_j}{\partial x_i}\right) \quad i,j = x,y,z \quad (2b)$$

$$\varepsilon_{ij}^{*} = \frac{1}{2}\left(\frac{\partial U_k}{\partial x_i}\frac{\partial U_k}{\partial x_j}\right) \quad i,j,k = x,y,z \quad (2c)$$

ε_{ij}^{l} denotes the linear parts and ε_{ij}^{*} the quadratic non-linear parts. Using the displacement field given in Eq. (1), the non-zero constituents of linear and non-linear parts of strain-displacement are derived as

$$\varepsilon_{xx}^{l} = \frac{\partial U}{\partial x} = u_0' - yv'' - zw'' - \omega\theta''$$

$$\varepsilon_{xy}^{l} = \frac{1}{2}\left(\frac{\partial U}{\partial y} + \frac{\partial V}{\partial x}\right) = -\frac{1}{2}\left(z + \frac{\partial \omega}{\partial y}\right)\theta' \quad (3a)$$

$$\varepsilon_{xz}^{l} = \left(\frac{\partial U}{\partial z} + \frac{\partial W}{\partial x}\right) = \frac{1}{2}\left(y - \frac{\partial \omega}{\partial z}\right)\theta'$$

$$\varepsilon_{xx}^{*}=\frac{1}{2}\left((\frac{\partial V}{\partial x})^{2}+(\frac{\partial W}{\partial x})^{2}\right)=\frac{1}{2}\left[v'^{2}+w'^{2}+r^{2}\theta'^{2}\right]$$
$$+yw'\theta'-zv'\theta'$$
$$\varepsilon_{xy}^{*}=\frac{1}{2}\left(\frac{\partial V}{\partial x}\frac{\partial V}{\partial y}+\frac{\partial W}{\partial x}\frac{\partial W}{\partial y}\right)=\frac{1}{2}\left(w'+\theta' y\right)\theta \quad (3b)$$
$$\varepsilon_{xz}^{*}=\frac{1}{2}\left(\frac{\partial V}{\partial x}\frac{\partial V}{\partial z}+\frac{\partial W}{\partial x}\frac{\partial W}{\partial z}\right)=-\frac{1}{2}\left(v'+\theta' z\right)\theta$$

In Eq. (3b), the term r^2 represents y^2+z^2.

The resultants of classical stresses for beams with doubly-symmetric I-section can be expressed as follows [26]

$$\left(N, M_y, M_z, B_\omega\right)=\int_A \sigma_{xx}\left(1, z, -y, -\omega\right)dA$$
$$M_{sv}=\int_A\left(\sigma_{xz}(y-\frac{\partial\omega}{\partial z})-\sigma_{xy}(z+\frac{\partial\omega}{\partial y})\right)dA \quad (4)$$

where N is the axial force. M_y and M_z denote the bending moments about major and minor axes, respectively. B_ω is the bi-moment. M_{sv} is the St-Venant torsion moment. The present model is applied in the case of balanced and symmetrical lay-ups of the web and both flanges. In the context of classical laminated plate theory and substitution Eq. (3a) into Eq. (4), the stress resultants of symmetrically balanced laminates are derived in terms of displacement components as [3]

$$N=(EA)_{com}u_0';\ M_z=(EI_z)_{com}v'';$$
$$M_y=-(EI_y)_{com}w'';\ B_\omega=(EI_\omega)_{com}\theta'';$$
$$M_{sv}=(GJ)_{com}\theta' \quad (5)$$

where $(EA)_{com}$ denotes axial rigidity. $(EI_y)_{com}$ and $(EI_z)_{com}$ represent the flexural rigidities of the y- and z-axes, respectively. $(EI_\omega)_{com}$ and $(GJ)_{com}$ are, respectively, warping and torsional rigidities of composite thin-walled beams with doubly symmetric I-section, defined by:

$$(EA)_{com}=2b_f A_{11}^{f}+dA_{11}^{w};$$
$$(EI_z)_{com}=2\frac{b_f^3}{12}A_{11}^{f}+dD_{11}^{w}$$
$$(EI_y)_{com}=2b_f D_{11}^{f}+2\frac{d^2}{4}b_f A_{11}^{f}+\frac{d^3}{12}A_{11}^{w} \quad (6)$$
$$(EI_\omega)_{com}=2(\frac{d^2}{4}A_{11}^{f}+D_{11}^{f})\frac{b_f^3}{12}+\frac{d^3}{12}D_{11}^{w};$$
$$(GJ)_{com}=4(2b_f D_{66}^{f}+dD_{66}^{w})$$

That indexes f and w refer to the web and the flange of the beam cross-section, respectively. A_{ij} and D_{ij} are the matrices of extensional and bending stiffness, respectively. These stiffness quantities for composite multi-layer I-section could be calculated as:

$$(A_{ij}^{f}, D_{ij}^{f})=\int Q_{ij}^{f}(1, z^2)dz \quad (7a)$$
$$(A_{ij}^{w}, D_{ij}^{w})=\int Q_{ij}^{w}(1, y^2)dy \quad (7b)$$

where Q_{ij}^{f} and Q_{ij}^{w} are the transformed reduced stiffness related to the flanges and web, respectively. In this research, equilibrium equations and boundary conditions are derived from stationary conditions of the total potential energy. Based on this principle, the following relation is obtained

$$\delta\Pi=\delta U_l+\delta U_0-\delta W_e=0 \quad (8)$$

In this formulation, δ denotes a variational operator. U_l and U_0 represent the elastic strain energy and the strain energy due to effects of the initial stresses, respectively. W_e denotes work done by external applied loads. δU_l could be computed using the following equation

$$\delta U_l=\int_V \sigma_{ij}\delta\varepsilon_{ij}^{l}dV=\int_0^L\int_A \sigma_{xx}\delta\varepsilon_{xx}^{l}dAdx$$
$$+2\int_0^L\int_A \sigma_{xy}\delta\varepsilon_{xy}^{l}dAdx+2\int_0^L\int_A \sigma_{xz}\delta\varepsilon_{xz}^{l}dAdx \quad (9)$$

in which, L expresses the element length. $\delta\varepsilon_{ij}^{l}$ is the variation of the linear parts of strain tensor. Using Eq. (3a), the variation of the linear part of strain tensor components is given by:

$$\delta\varepsilon_{xx}^{l}=\delta u_0'-y\,\delta v''-z\,\delta w''-\omega\delta\theta'';$$
$$\delta\varepsilon_{xz}^{l}=\frac{1}{2}\left(y-\frac{\partial\omega}{\partial z}\right)\delta\theta';$$
$$\delta\varepsilon_{xy}^{l}=-\frac{1}{2}\left(z+\frac{\partial\omega}{\partial y}\right)\delta\theta' \quad (10)$$

Substituting equation (10) into relation (9) and integrating over beam's cross-section, the expression of the strain energy variation can be carried out as:

$$\delta U_l=\int_0^L\int_A \sigma_{xx}\left(\delta u_0'-y\,\delta v''-z\,\delta w''-\omega\delta\theta''\right)dAdx$$
$$+\int_0^L\int_A \sigma_{xy}\left(-(z+\frac{\partial\omega}{\partial y})\delta\theta'\right)dAdx$$
$$+\int_0^L\int_A \sigma_{xz}\left((y-\frac{\partial\omega}{\partial z})\delta\theta'\right)dAdx \quad (11)$$
$$=\int_L\left(N\,\delta u_0'+M_z\delta v''-M_y\delta w''+B_\omega\delta\theta''\right)dx$$
$$+\int_0^L\left(M_{sv}\delta\theta'\right)dx$$

Substituting Eq. (5) into Eq. (11) yields:

$$\delta U_l=\int_L\begin{pmatrix}(EA)_{com}u_0'\delta u_0'+(EI_z)_{com}v''\delta v''\\+(EI_y)_{com}w''\delta w''\\+(EI_\omega)_{com}\theta''\delta\theta''+(GJ)_{com}\theta'\delta\theta'\end{pmatrix}dx \quad (12)$$

Also, the variation form of strain energy due to initial stresses can be stated as

$$\delta U_0=\int_V \sigma_{ij}^{0}\delta\varepsilon_{ij}^{*}dV=\int_0^L\int_A \sigma_{xx}^{0}\delta\varepsilon_{xx}^{*}dAdx$$
$$+2\int_0^L\int_A \sigma_{xy}^{0}\delta\varepsilon_{xy}^{*}dAdx+2\int_0^L\int_A \sigma_{xz}^{0}\delta\varepsilon_{xz}^{*}dAdx \quad (13)$$

In Eq. (13), σ_{xy}^{0} and σ_{xz}^{0} indicate the mean values of the shear stress and σ_{xx}^{0} signifies initial normal stress in the cross-section. According to Fig. 1, it is contemplated that the external bending moment occurs about the major principal axis (M_y^{*}). Therefore, the magnitude of bending moment with respect to z-axis is equal to zero. Regarding this, the most general case of normal and shear stresses associated the external bending moment M_y^{*} and shear force V_z are considered as:

$$\sigma_{xx}^{0}=-\frac{M_y^{*}}{I_y}z;\ \sigma_{xz}^{0}=\frac{V_z}{A}=-\frac{M_y^{*\prime}}{A};\ \sigma_{xy}^{0}=0 \quad (14)$$

Based on Eq. (3b), the first variation of non-linear strain-displacement relations can be written as:

$$\begin{aligned}\delta\varepsilon_{xx}^{*} &= v'\delta v' + w'\delta w' + r^{2}\theta'\delta\theta' + yw'\delta\theta' \\ &\quad + y\theta'\delta w' - z\theta'\delta v' - zv'\delta\theta' \\ \delta\varepsilon_{xy}^{*} &= \frac{1}{2}\left(\delta w' + y\,\delta\theta'\right)\theta + \frac{1}{2}\left(w' + y\theta'\right)\delta\theta \\ \delta\varepsilon_{xz}^{*} &= -\frac{1}{2}\left(\delta v' + z\,\delta\theta'\right)\theta - \frac{1}{2}\left(v' + \theta' z\right)\delta\theta\end{aligned} \tag{15}$$

Substituting equations (14) and (15) into relation (13) yields:

$$\begin{aligned}\delta U_{0} = \int_{0}^{L}\int_{A}\left(-\frac{M_{y}^{*}}{I_{y}}z\right)\begin{pmatrix} v'\delta v' + w\,\delta w' \\ + r^{2}\theta'\delta\theta' \\ + y\theta'\delta w' + yw'\delta\theta' \\ - z\theta'\delta v' - zv'\delta\theta'\end{pmatrix}dA\,dx \\ + \int_{0}^{L}\int_{A}\left(-\frac{M_{y}^{*\prime}}{A}\right)\begin{pmatrix} -\theta\delta v' - v'\delta\theta \\ -z\,\theta\delta\theta' - z\,\theta'\delta\theta\end{pmatrix}dA\,dx\end{aligned} \tag{16}$$

In this stage, by integrating Eq. (16) over the cross-section area of the beam, the final form of the variation of strain energy due to the initial stresses is acquired as

$$\delta U_{0} = \int_{0}^{L}\left(-M_{y}^{*}v''\delta\theta - M_{y}^{*}\theta\delta v''\right)dx \tag{17}$$

The first variation of external load work (W_e) of the beam under distributed vertical forces q_z applied along a line (PP′) on the section contour (Fig. 1a) can be written in the form of

$$\delta W_{e} = \int_{0}^{L} q_{z}\,\delta w_{P}\,dx \tag{18}$$

In Eq. (18), w_P is the vertical displacement of point P. According to kinematics used in Asgarian et al. [34] and by adopting the quadratic approximation, the vertical displacement of the point P and its first variation are as follows:

$$w_{P} = w - z_{P}\frac{\theta^{2}}{2} \rightarrow \delta w_{P} = \delta w - z_{P}\theta\delta\theta \tag{19a, b}$$

In this equation, z_P is used to imply the eccentricity of the applied loads from the centroid of the cross-section. Substituting Eq. (19b) into Eq. (18) yields

$$\delta W_{e} = \int_{0}^{L}\left(q_{z}\delta w - M_{t}\theta\delta\theta\right)dx \tag{20}$$

in which, $M_{t} = q_{z}z_{P}$ denotes the second order torsion moment due to load eccentricity.

After inserting Eq. (12), (16) and (20) into Eq. (8), the expression of the firs variation of total potential energy can be written as

$$\begin{aligned}\delta\Pi = \int_{L}\begin{pmatrix}(EA)_{com}u_{0}'\delta u_{0}' + (EI_{z})_{com}v''\delta v'' \\ + (EI_{y})_{com}w''\delta w'' \\ + (EI_{\omega})_{com}\theta''\delta\theta'' + (GJ)_{com}\theta'\delta\theta'\end{pmatrix}dx \\ + \int_{0}^{L}\left(-M_{y}^{*}v''\delta\theta - M_{y}^{*}\theta\delta v''\right)dx \\ - \int_{0}^{L}\left(q_{z}\delta w - M_{t}\theta\delta\theta\right)dx = 0\end{aligned} \tag{21}$$

Based on the equation presented above, the first variation of the total potential energy contains the virtual displacements ($\delta u, \delta v, \delta w, \delta\theta$) and their derivatives. After appropriate integrations by parts, and after mathematical simplifications, we get the following equilibrium equations in the stationary state

$$((EA)_{com}u_{0}')' = 0 \tag{22a}$$

$$\left((EI_{y})_{com}w''\right)'' = q_{z} \tag{22b}$$

$$\left((EI_{z})_{com}v''\right)'' - \left(M_{y}^{*}\theta\right)'' = 0 \tag{22c}$$

$$\left((EI_{\omega})_{com}\theta''\right)'' - \left((GJ)_{com}\theta'\right)' - M_{y}^{*}v'' + M_{t}\theta = 0 \tag{22d}$$

The related boundary conditions at the ends of balanced laminated beam with thin-walled cross-section can be expressed as

$$(EA)_{com}u_{0}' = 0 \quad \text{or} \quad \delta u_{0} = 0 \tag{23a}$$

$$(EI_{z})_{com}v'' = 0 \quad \text{or} \quad \delta v' = 0 \tag{23b}$$

$$((EI_{z})_{com}v'')' - (M_{y}^{*}\theta)' = 0 \quad \text{or} \quad \delta v = 0 \tag{23c}$$

$$(EI_{y})_{com}w'' = 0 \quad \text{or} \quad \delta w' = 0 \tag{23d}$$

$$((EI_{y})_{com}w'')' = 0 \quad \text{or} \quad \delta w = 0 \tag{23e}$$

$$(EI_{\omega})_{com}\theta'' = 0 \quad \text{or} \quad \delta\theta' = 0 \tag{23f}$$

$$((EI_{\omega})_{com}\theta'')' - (GJ)_{com}\theta' = 0 \quad \text{or} \quad \delta\theta = 0 \tag{23g}$$

In the equilibrium equations, the first and second ones are uncoupled and stable, and do not affect the lateral buckling behavior of I-beam subjected to transverse loading. The differential equations (22c, d) have a coupled nature due to the presence of the lateral deflection v and torsion θ component, as well as the bending moment M_{y}^{*}. Based on the straightforward methodology presented by Soltani et al. [34-36], the governing equilibrium equation for the lateral displacement (22b) can be rewritten as

$$v'' = \frac{M_{y}^{*}\theta}{(EI_{z})_{com}} \tag{24}$$

whose substitution in the fourth equilibrium Eq. (22d) enables its redefinition in an uncoupled form as only dependent on the twist angle θ, independent from the lateral displacement v, i.e.

$$\left((EI_{\omega})_{com}\theta''\right)'' - \left((GJ)_{com}\theta'\right)' - \frac{M_{y}^{*2}\theta}{(EI_{z})_{com}} + M_{t}\theta = 0 \tag{25}$$

Eqs. (23f) and (23g) are the corresponding boundary conditions of the resulting formulation.

Since the flanges and/or web are variable, all stiffness quantities of the composite beam are functions of the x-coordinate. In this regard, the solution of the resulting fourth-order differential equation in terms of the twist angle (25) is not straightforward and only analytical or numerical techniques such as Galerkin's or Rayleigh-Ritz methods [37-39], the finite difference method [40, 41], the differential quadrature method [26, 36, 42, 43], and the power series method [44-46] are feasible. In the present work, Galerkin's method as a highly accurate analytical methodology is used to solve Eq. (25) and obtain the lateral buckling load. Additionally, this analytical approach is one of the most easy-to-apply methodologies to exactly determine the lateral stability strength of unrestrained and braced continuous structural elements. Based on the assumptions of this technique, the differential equilibrium

equations and approximate displacement functions are required. Note that the assumed buckled deformations should satisfy the geometric boundary conditions of the beam. It is also necessary to mention that the resulting fourth-order differential equation (Eq. (25)) is applicable for lateral stability analysis of composited tapered I-beams that are restrained from the torsion at their ends ($\theta(0)=\theta(L)=0$).

For simply supported beams with free warping at both ends ($\theta''(0)=\theta''(L)=0$), the twist angle also equals zero ($\theta(0)=\theta(L)=0$). For this condition, the first displacement mode in torsion after lateral buckling can be thus approximated by trigonometric function as [38, 39]

$$\theta(x)=\theta_1 \sin\left(\frac{\pi x}{L}\right) \tag{26}$$

In the case of fixed-fixed members, both supports are prevented from freely warping. Therefore, the twist angle and the rate of twist at the fixed ends are restrained ($\theta(0)=\theta(L)=\theta'(0)=\theta'(L)=0$). The expression for the angle of twist can be approximated as [38, 39]

$$\begin{aligned}\theta(x)&=\theta_1\left(1-\cos\left(\frac{2\pi x}{L}\right)\right)\\&+\theta_2\left(1-\cos\left(\frac{3\pi x}{L}\right)\right)+\theta_3\left(1-\cos\left(\frac{5\pi x}{L}\right)\right)\end{aligned} \tag{27}$$

For the fixed-simply supported I-beams, the left end (fixed one) of the beam are prevented from freely warping ($\theta(0)=\theta'(0)=0$), while, the right end of the element is free to warp but restrained from the torsion ($\theta(0)=\theta''(L)=0$). One gets [38, 39]:

$$\begin{aligned}\theta(x)&=\theta_1\left(\left(\frac{x}{L}\right)^4-2.5\left(\frac{x}{L}\right)^3+1.5\left(\frac{x}{L}\right)^2\right)\\&+\theta_2\begin{pmatrix}\sin\left(\frac{kx}{L}\right)-k\left(\frac{x}{L}\right)\\+k\cos\left(\frac{kx}{L}-k\right)\end{pmatrix}\end{aligned} \tag{28}$$

where $\theta_i\,(i=1,2,3)$ is the associated displacement amplitude.

In the current work, only simply supported beam with free warping and bending at both ends is considered. Following the rules of Galerkin's method and by substituting the buckled shape function and its derivatives into Eq. (25) one gets

$$\begin{aligned}&\int_L\left(\left(\frac{\pi}{L}\right)^2\frac{M_y^{*2}}{(EI_z)_{com}}+z_p q_z\right)\left(\sin\left(\frac{\pi x}{L}\right)\right)^2 dx\\&=\int_L\begin{pmatrix}\left(\frac{\pi}{L}\right)^2\left((EI_\omega)_{com}\sin\left(\frac{\pi x}{L}\right)\right)''\sin\left(\frac{\pi x}{L}\right)\\-\left(\frac{\pi}{L}\right)\left((GJ)_{com}\cos\left(\frac{\pi x}{L}\right)\right)'\sin\left(\frac{\pi x}{L}\right)\end{pmatrix}dx\end{aligned} \tag{29}$$

By substituting the required stiffness coefficients as well as the bending and torsion moments expressions into the formulation presented above following an appropriate mathematical procedure, the lateral-torsional buckling load can be acquired.

3. Findings and Discussion

In the preceding section, an analytical methodology has been formulated to calculate the lateral-torsional buckling loads of thin-walled fiber metal laminates beam with varying I-section. In this section, a comprehensive example is conducted to show the effects of significant parameters such as laminate stacking sequences, metal volume fraction, loading position, and web tapering ratio on the lateral buckling capacity of multi-layered composite tapered I-beam. In this regard, the linear lateral buckling analysis is performed for a simply supported 10-layer FML web tapered I-beam with a span of 10m. All section walls (both flanges and web) are laminated symmetrically concerning its mid-plane and made of Aluminum alloy 2024-T3 (outer metal layers) and E-glass/epoxy material (eight inner composite layers). The material features of the lamina are as follows [25]: for the aluminum plies, E = 72.4 GPa and υ = 0.33; and for the fiber-reinforced composite layers, E_x = 38.6 GPa, E_y = 8.27 GPa, Gxy = 4.14 GPa, and υxy = 0.26.

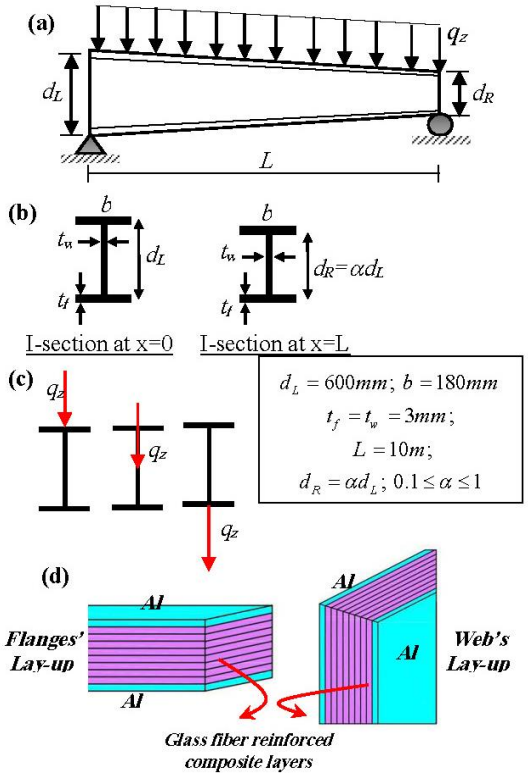

Fig. 2: Simply supported FML I-beam with varying cross-section subjected to uniformly distributed load: Geometrical properties, loading position, and web and flanges lay-up arrangement

As shown in Figure 2, at the left end section, both flanges are assumed to be 180mm wide (b_f), and the web of the I-shape is 600mm deep (d_L). It is also supposed that the web height of the I-section at the left end (d_L) is made to diminish linearly to (d_R) at the right one (Figure 2). Therefore, the web tapering ratio is defined as $\alpha = d_R / d_L$: Note that this parameter (α) is a non-negative variable and can change from 0.1 to 1.0. Moreover, I-beam with a uniform cross-section is achieved when the mentioned

parameter (α) equals one. For the above case, the required stiffness quantities presented in Eq. (6) can be rewritten as follows:

$$
\begin{aligned}
(EI_z)_{com} &= \frac{1}{6} b_f A_{11}^f + \left(d_L(\alpha-1)(\frac{x}{L}) + d_L \right) D_{11}^w \\
(EI_\omega)_{com} &= \frac{1}{6} b_f{}^3 D_{11}^f \\
&+ \frac{1}{24} \left(d_L(\alpha-1)(\frac{x}{L}) + d_L \right)^2 b_f{}^3 A_{11}^f \\
&+ \frac{1}{12} \left(d_L(\alpha-1)(\frac{x}{L}) + d_L \right)^3 D_{11}^w \\
(GJ)_{com} &= 8 b_f D_{66}^f + 4 \left(d_L(\alpha-1)(\frac{x}{L}) + d_L \right) D_{66}^w
\end{aligned}
\tag{30}
$$

As shown in Fig. 2, the selected simply supported web-tapered beam is subjected to uniformly distributed load. For this loading case, the internal bending moment in the beam equals

$$M_y^* = q_z \frac{L^2}{2} (\frac{x}{L} - \frac{x^2}{L^2}) \tag{31}$$

The uniformly transverse load is also supposed to be applied at three different positions: the top flange, the centroid (shear center), and the bottom flange. The load height parameter (z_P) and, consequently, the second-order torsion moment can be written as:

$$
\begin{aligned}
z_P &= 0.5 \left(d_L(\alpha-1)(\frac{x}{L}) + d_L \right) \\
M_t &= 0.5 q_z \left(d_L(\alpha-1)(\frac{x}{L}) + d_L \right)
\end{aligned}
\tag{32}
$$

Finally, the solution of Eq. (26) concerning transverse load q_z, leads to the determination of the lateral buckling loads for the considered case by inserting the stiffness coefficients Eq. (30) and taking into account formulas (31-32).

The next part is divided into two different subsections; the first one for verification of the formulation proposed herein, and the latter aims to peruse the influence of the above-mentioned factors on the linear lateral buckling behavior of the considered member.

Before presenting the results, it is important to note that shear deformations are neglected and the laminate consists of perfectly bonded layers. Additionally, based on Vlasov's model, the cross-section is rigid in its own plane and consequently, no distortional deformations occur. This means that only overall buckling occurs.

3.1. Verification

As far as the authors know, no numerical and/or experimental studies have been published on the linear buckling analysis of thin-walled FML profile under transverse loading. Therefore, to investigate the accuracy of the formulation presented herein, the obtained results have been compared with those acquired with the finite element method, using ANSYS code. To that end, Table 1 gives the estimated values of the lateral buckling load (q_{cr}) of the contemplated beam with variable thin-walled I-section for different tapering parameters ($\alpha = 1$, 0.8, 0.6, 0.5, and 0.3) by assuming MVF=0.2 when transverse loading is applied at the mid-height along the beam length. In this section, the web and flanges are assumed to have identical stacking sequences. The abovementioned thin-walled FML beams have been modeled using SHELL281 of ANSYS software. This element is suitable for analyzing thin to moderately-thick shell structures. SHELL281 has eight nodes with six degrees of freedom at each node: translations in the x, y, and z axes, and rotations about the x, y, and z-axes [47]. In all developed ANSYS models in this study, the applied aspect ratio of the mesh (length-to-maximum width) was close to unity at the bigger cross-section. In order to model pinned end condition, lateral and vertical displacements are null in both ends of the beam but flexural rotations and warping are free along the beam length. In order to restrain the beam from axial displacement, the longitudinal translation is prevented in one node at one of the end section. Fig. 3 shows the overall lateral buckling mode shape of uniform beam (a=1) and tapered one (α=0.6) having unidirectional ([Al, $(0)_7$]$_S$) stacking sequence.

(a) 1st buckling mode shape for prismatic beam (α=1)

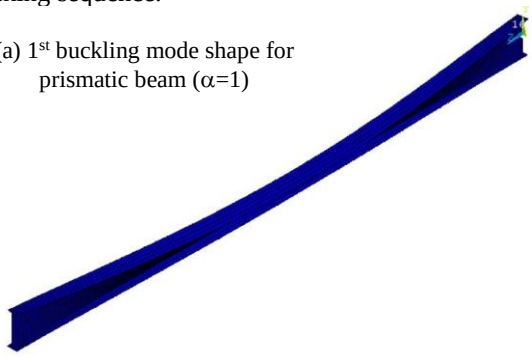

(b) 1st buckling mode shape for tapered beam (α=0.6)

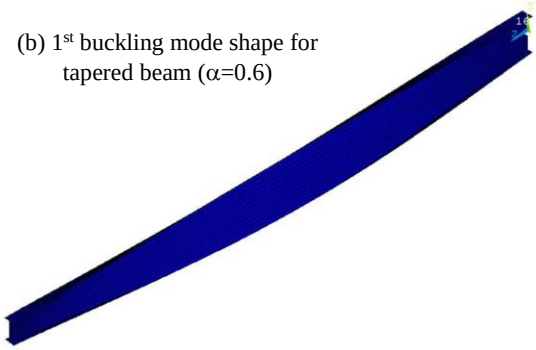

Fig. 3: The uniform shell mesh used for FML beam with doubly-symmetric I-section subjected to uniformly distributed load on the centroid

Additionally, the relative errors (Δ) associated with the present approach are given in Table 1 by the following expression:

$$\Delta = \frac{\left| q_{cr}^{Galerkin} - q_{cr}^{ANSYS} \right|}{q_{cr}^{ANSYS}} \times 100 \tag{33}$$

Table. 1: The lateral buckling loads comparison between the present methodology and ANSYS code for distributed load applied at the centroid when MVF=0.2

Stacking sequence	α	Present	ANSYS	Δ(%)
[Al, $(0)_4$]$_S$	1	389.316	365.096	6.221

	0.8	353.136	330.687	6.357
	0.6	317.759	297.862	6.262
	0.5	300.461	279.285	7.048
	0.3	266.895	243.753	8.671
[Al, (90)$_4$]$_s$	1	197.155	189.697	3.782
	0.8	180.010	171.969	4.467
	0.6	163.291	155.618	4.699
	0.5	155.133	146.563	5.524
	0.3	139.339	130.060	6.660

Table 1 shows that the critical load values calculated using the proposed technique are in good agreement with the results obtained by modeling in finite element software so that the error rate is less than 10%.

3.2. Parametric Study

After validating and verifying the methodology proposed herein, the impact of metal volume fraction on lateral stability capacity will be assessed in the following Section. The main objective of the current part is also to find out the optimal laminate stacking sequence of the inner composite layers of simply supported FML web-tapered I-beam under uniformly distributed load that gives the highest lateral-torsional buckling resistance. In this regard, twelve different practical stacking sequences (Table 2) are considered. Note that the material for all the inner plies is E-glass/epoxy.

Table. 2: Stacking sequence for doubly-symmetric I-section

No.	Top and bottom flanges	Web
1	$[Al,(0/90)_2]_s$	$[Al,(\pm45)_2]_s$
2	$[Al,(0/90)_2]_s$	$[Al/0/\pm45/0]_s$
3	$[Al,(0/90)_2]_s$	$[Al/90/\pm45/90]_s$
4	$[Al,(0/90)_2]_s$	$[Al,(0/90)_2]_s$
5	$[Al/0_3/90]_s$	$[Al,(\pm45)_2]_s$
6	$[Al/0_3/90]_s$	$[Al/0/\pm45/0]_s$
7	$[Al/0_3/90]_s$	$[Al/90/\pm45/90]_s$
8	$[Al/0_3/90]_s$	$[Al/0_3/90]_s$
9	$[Al/0_4]_s$	$[Al,(\pm45)_2]_s$
10	$[Al/0_4]_s$	$[Al/0/\pm45/0]_s$
11	$[Al/0_4]_s$	$[Al/90/\pm45/90]_s$
12	$[Al/0_4]_s$	$[Al/0_4]_s$

In Figs. 4-6, we plot the variations of the lowest lateral buckling load variations versus the metal volume fraction (varying from 0 to 1.0) for different laminate stacking sequences and web-tapering parameters, and for the three different load positions, namely the top flange, the centroid and the bottom flange, respectively.

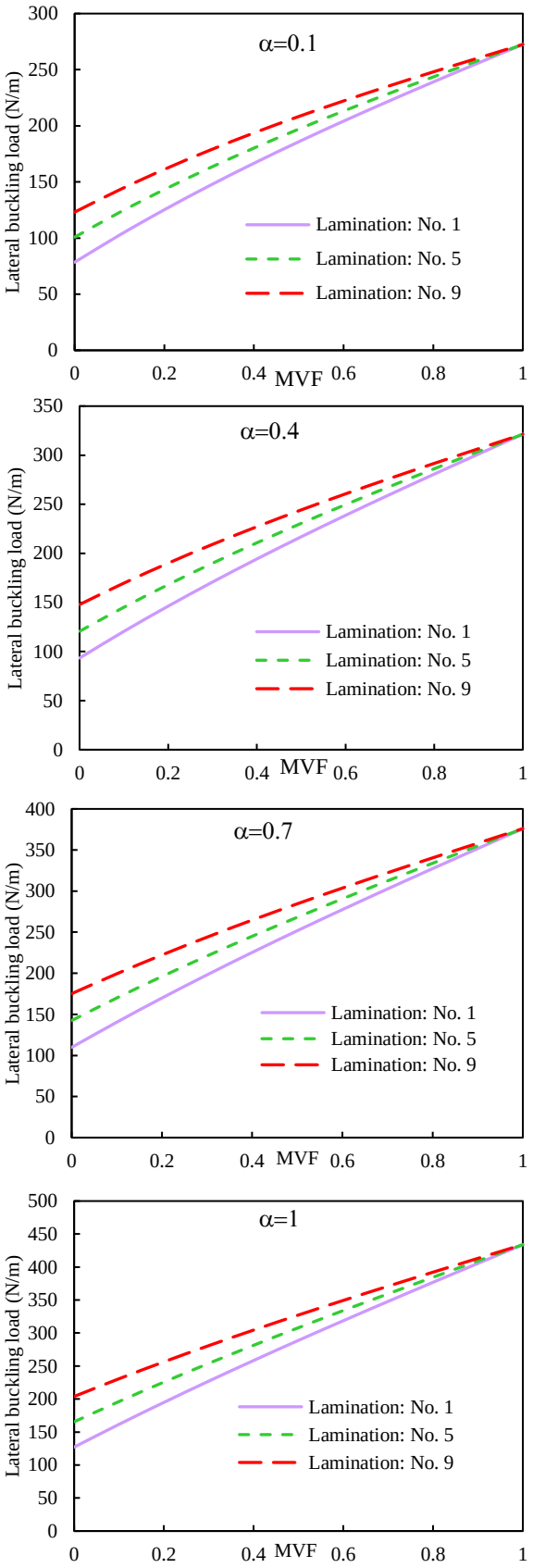

Fig. 4: Variation of the lateral buckling load with respect to metal volume fraction change: effect of different sequences of laminations, for different tapering ratios, and for a transverse load applied on the top flange

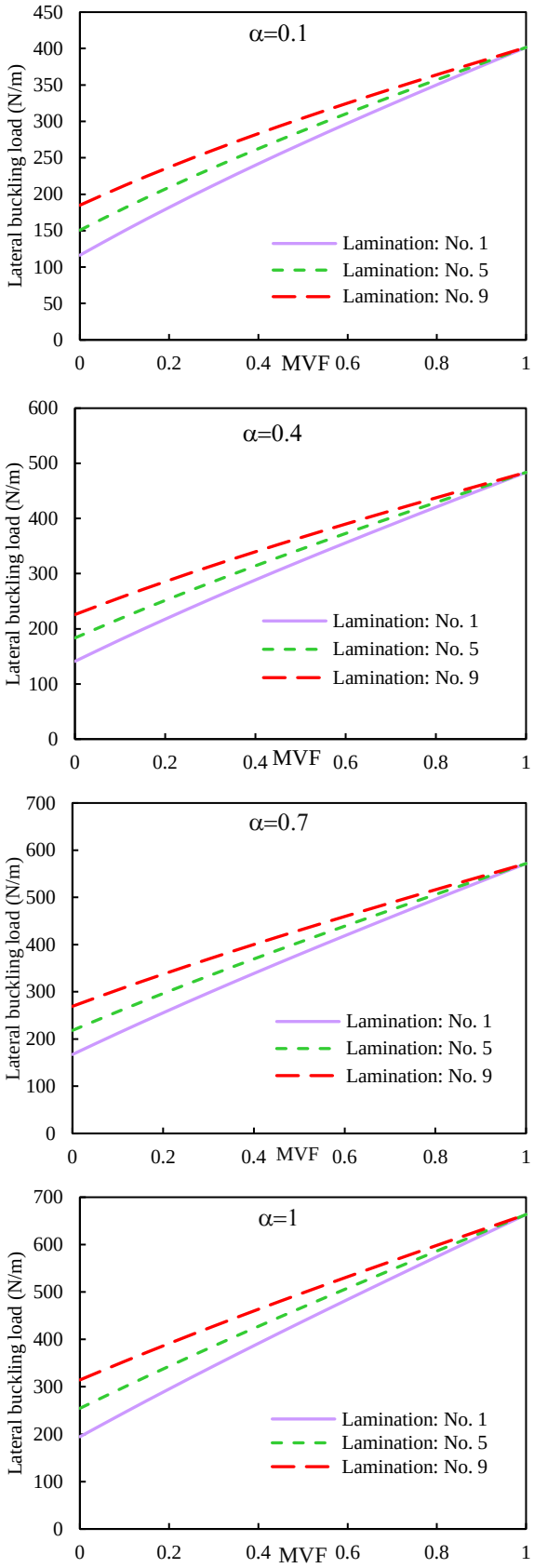

Fig. 5: Variation of the lateral buckling load with respect to metal volume fraction change: effect of different sequences of laminations, for different tapering ratios, and for a transverse load applied at the centroid

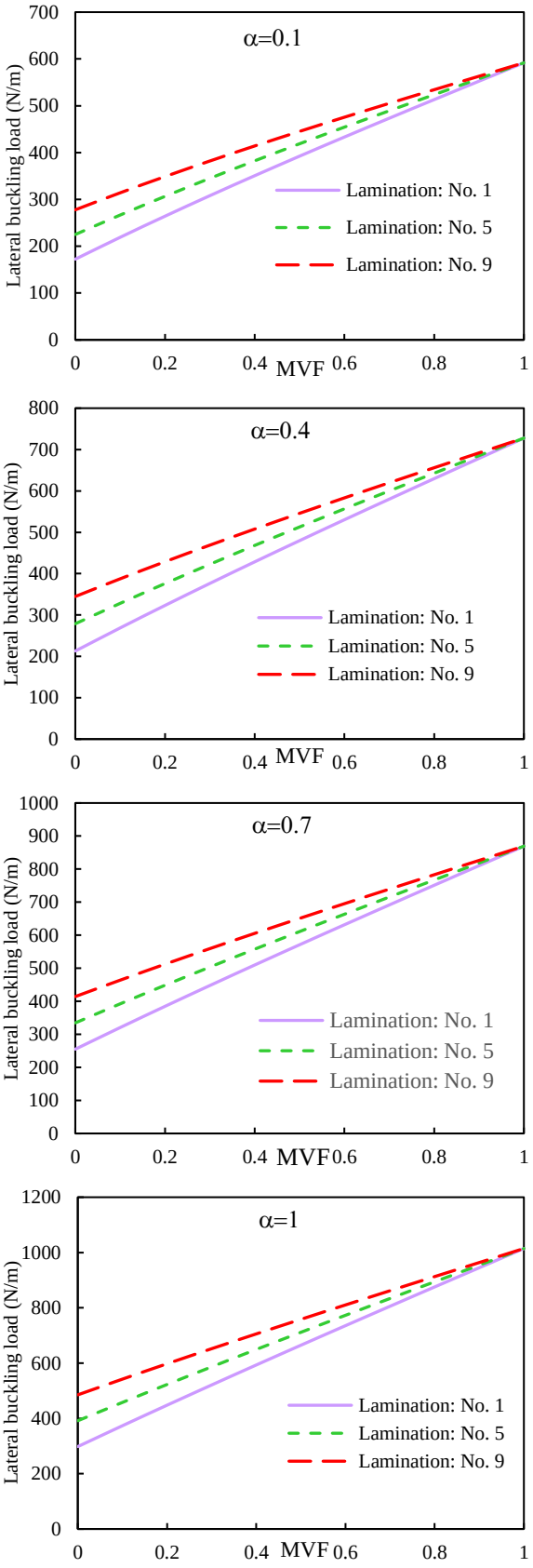

Fig. 6: Variation of the lateral buckling load with respect to metal volume fraction change: effect of different sequences of laminations, for different tapering ratios, and for a transverse load applied on the bottom flange

Table. 3: Metal volume fraction and tapering parameter effects on the lateral-torsional buckling load (q_{nor}) of simply supported thin-walled FML beam with different sequences of lamination (transverse load on the top flange).

Stacking sequence	α=0.4			α=0.7			α=1		
	MVF=0	MVF=0.4	MVF=0.6	MVF=0	MVF=0.4	MVF=0.6	MVF=0	MVF=0.4	MVF=0.6
No. 2	91.168	193.828	238.575	107.574	224.847	277.311	124.895	257.907	318.563
No. 3	92.916	194.189	238.683	109.355	225.219	277.421	126.688	258.283	318.675
No. 4	89.651	193.518	238.483	106.030	224.528	277.215	123.339	257.582	318.466
No. 6	118.413	210.274	249.531	140.234	244.516	290.417	163.243	280.971	333.934
No. 7	120.185	210.638	249.639	142.033	244.890	290.528	165.051	281.350	334.046
No. 8	116.888	209.963	249.438	138.686	244.196	290.322	161.688	280.648	333.838
No. 10	145.643	226.701	260.480	172.822	264.171	303.518	201.582	304.025	349.301
No. 11	147.429	227.067	260.588	174.693	264.546	303.629	203.399	304.405	349.414
No. 12	144.109	226.388	260.387	171.327	263.849	303.422	200.021	303.700	349.205

Table. 4: Metal volume fraction and tapering parameter effects on the lateral-torsional buckling load (q_{nor}) of simply supported thin-walled FML beam with different sequences of lamination (transverse load on the centroid).

Stacking sequence	α=0.4			α=0.7			α=1		
	MVF=0	MVF=0.4	MVF=0.6	MVF=0	MVF=0.4	MVF=0.6	MVF=0	MVF=0.4	MVF=0.6
No. 2	138.609	288.060	355.653	164.900	338.418	418.455	192.187	390.960	483.957
No. 3	140.502	288.448	355.769	166.830	338.818	418.574	192.128	391.365	484.077
No. 4	136.959	287.725	355.553	163.213	338.072	418.352	190.485	390.607	483.852
No. 6	180.996	313.618	372.681	215.901	369.112	438.909	252.102	426.981	507.964
No. 7	182.918	314.010	372.798	217.855	369.515	439.029	254.063	427.389	508.086
No. 8	179.336	313.283	372.582	214.214	368.767	438.807	250.408	426.631	507.860
No. 10	233.363	339.152	389.701	266.885	399.788	459.358	312.004	462.988	531.967
No. 11	225.303	339.547	389.818	268.855	400.194	459.478	313.978	463.398	532.089
No. 12	221.691	338.815	389.601	265.189	399.441	459.255	310.303	462.636	531.863

Table. 5: Metal volume fraction and tapering parameter effects on the lateral-torsional buckling load (q_{nor}) of simply supported thin-walled FML beam with different sequences of lamination (transverse load on the bottom flange).

Stacking sequence	α=0.4			α=0.7			α=1		
	MVF=0	MVF=0.4	MVF=0.6	MVF=0	MVF=0.4	MVF=0.6	MVF=0	MVF=0.4	MVF=0.6
No. 2	210.737	428.105	530.186	252.776	509.354	631.439	295.735	592.654	735.221
No. 3	212.457	428.460	530.291	254.515	509.716	631.547	297.470	593.018	735.330
No. 4	209.223	427.795	530.093	251.236	509.035	631.344	294.184	592.330	735.125
No. 6	276.654	467.754	556.610	332.395	557.198	663.328	389.328	648.866	772.691
No. 7	278.397	468.112	556.716	334.153	557.563	663.437	391.080	649.232	772.800
No. 8	275.147	467.447	556.519	330.873	556.884	663.235	387.809	648.550	772.597
No. 10	342.556	507.384	583.028	412.002	605.028	695.213	482.913	705.067	810.157
No. 11	344.314	507.745	583.134	413.771	605.395	695.322	484.673	705.435	810.266
No. 12	341.041	507.075	582.936	410.474	604.712	695.119	481.389	704.750	810.063

At the same time, the magnitude of the lateral-torsional buckling load (q_{cr}) for various lay-up arrangements, and three different web-tapering parameters (α= 0.4, 0.7 and 1) with different metal volume fractions (MVF=0.0, 0.4 and 0.6) are listed in Tables 3-5. The contribution of load height position from the cross-section centroid on the lateral buckling strength is also taken into account. The resulting lateral buckling loads are respectively illustrated in Tables 3 and 4 for load positions on the top flange and the shear center and Table 5 for the bottom flange load position.

Based on the presented results, the endurable lateral buckling increases significantly with increasing the volume fraction of the metal. This result is predictable based on the material properties of E-glass/epoxy and aluminum. It should be noted that MVF=0 represents full fiber composite I-section in the absence of metal layers, and MVF=1 indicates that all cross-section walls are entirely made of aluminum. Also, according to these illustrations, it can be stated that as the percentage of aluminum increases, the effect of laminations on the lateral stability of FML web-tapered I-beam under transverse load decreases significantly. This trend can be explained based on the principle that the participation of glass fiber layers in determining lateral buckling strength decreases by increasing the volume fraction of metal. This is due to thickening aluminum sheets and thinning fiber reinforced epoxy composite layers.

Moreover, it is seen that the uniformly transverse load position has a significant effect on the stability strength of unrestrained laminated composite beams with varying doubly-symmetric I-section. For these loading cases, the lateral buckling strength will be improved when the distributed load location is on the bottom flange due to the reduced rotation of the I-section from its original, and the lower values are obtained when the load is applied on the top flange position. Note also that the web non-uniformity parameter has a considerable impact on the lateral-

torsional buckling strength. The tapering parameter weakens the web-tapered beam due to decreasing the member stiffness. Based on the results presented, it can be finally concluded that the optimum laminations for obtaining the highest lateral strength of simply supported web-tapered beam under distributed load are achieved by aligning the constituent fibers of both flanges at zero and the web fiber must be also placed at an angle of $\pm 45^{o}$ between two metal sheets. In this regard, Fig. 7 schematically shows the optimal lay-up arrangements of both flanges and the web of I-section by setting MVF=0.4.

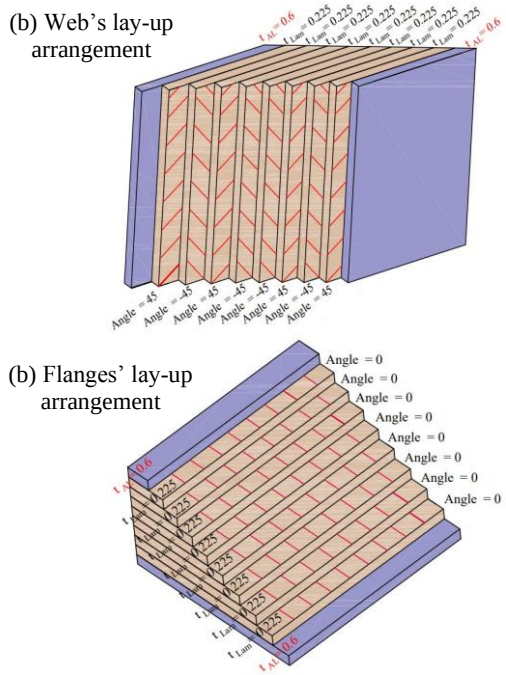

Fig. 7: Optimal ply stack of the web and both flanges (MVF=0.4)

4. Conclusions

The purpose of present paper is to investigate discrepancies between the elastic buckling behavior of fiber-metal laminate (FML) and composite thin-walled beam under transverse loading conditions. It is assumed that all section walls (the web and both flanges) are laminated symmetrically with respect to its mid-plane and consist of two metal layers at the outer sides of fiber reinforced epoxy composite laminates. The classical lamination theory conjugated with Vlasov's model assumptions were employed to determine the coupled governing differential equations for the lateral deflection and twist angle. The Galerkin's method is then employed for solving the resulting governing equations in term of the twist angle and boundary condition. In this research, glass/epoxy is considered for composite plies and aluminum for metal sheets. After verification with ANSYS software, the influence of several types of lay-up schemes, metal percentage, transverse loading position, and web tapering ratio on lateral-torsional stability strength of unrestrained simply supported composite 10-layer FML tapered I-beam is thoroughly measured. According to the numerical outcomes, it is concluded that the maximum lateral buckling load for simply supported FML web tapered I-beam subjected to uniformly distributed load is obtained by placing the fiber angle of each inner composite ply at $\pm 45^{o}$ in the web and 0^{o} in both flanges. It is also observed that the buckling capacity of simply supported laminated beam with doubly-symmetric I-section is best when the uniformly distributed load is applied on the bottom flange. Additionally, the results show that increasing the metal volume fraction leads to enhance linear buckling strength of glass-reinforced aluminum laminate I-beam under transverse loading. For the optimum laminate stacking sequence, the endurable lateral buckling load increases approximately 25% by raising the metal volume percentage from 0% to 20%.

References

[1] Rajasekaran, S. (1994). Instability of tapered thin-walled beams of generic section. Journal of engineering mechanics, 120(8), 1630-1640.
[2] Nam, H. W., Hwang, W., & Han, K. S. (2001). Stacking sequence design of fiber-metal laminate for maximum strength. Journal of Composite Materials, 35(18), 1654-1683.
[3] Lee, J., Kim, S. E., & Hong, K. (2002). Lateral buckling of I-section composite beams. Engineering Structures, 24(7), 955-964.
[4] Lee, J., & Kim, S. E. (2002). Free vibration of thin-walled composite beams with I-shaped cross-sections. Composite structures, 55(2), 205-215.
[5] Lee, J. (2005). Flexural analysis of thin-walled composite beams using shear-deformable beam theory. Composite Structures, 70(2), 212-222.
[6] Vo, T. P., & Lee, J. (2007). Flexural–torsional buckling of thin-walled composite box beams. Thin-walled structures, 45(9), 790-798.
[7] Oh, S. Y., Librescu, L., & Song, O. (2005). Vibration and instability of functionally graded circular cylindrical spinning thin-walled beams. Journal of sound and vibration, 285(4-5), 1071-1091.
[8] Rajasekaran, S., & Nalinaa, K. (2005). Stability and vibration analysis of non-prismatic thin-walled composite spatial members of generic section. International Journal of Structural Stability and Dynamics, 5(04), 489-520.
[9] Magnucka-Blandzi, E. (2009). Critical state of a thin-walled beam under combined load. Applied mathematical modelling, 33(7), 3093-3098.
[10] Vo, T. P., & Lee, J. (2009). Flexural–torsional coupled vibration and buckling of thin-walled open section composite beams using shear-deformable beam theory. International Journal of Mechanical Sciences, 51(9-10), 631-641.
[11] Moon, C. J., Kim, I. H., Choi, B. H., Kweon, J. H., & Choi, J. H. (2010). Buckling of filament-wound composite cylinders subjected to hydrostatic pressure for underwater vehicle applications. Composite Structures, 92(9), 2241-2251.
[12] Ascione, L., Berardi, V. P., Giordano, A., & Spadea, S. (2013). Local buckling behavior of FRP thin-walled beams: a mechanical model. Composite Structures, 98, 111-120.
[13] Araújo, A. L., Carvalho, V. S., Soares, C. M., Belinha, J., & Ferreira, A. J. M. (2016). Vibration analysis of laminated soft core sandwich plates with piezoelectric sensors and actuators. Composite Structures, 151, 91-98.
[14] Ravishankar, H., Rengarajan, R., Devarajan, K., & Kaimal, B. (2016). Free vibration bahaviour of fiber metal

laminates, hybrid composites, and functionally graded beams using finite element analysis. International Journal of Acoustics and Vibration, 21(4), 418-428.

[15] Banat, D., Kolakowski, Z., & Mania, R. J. (2016). Investigations of FML profile buckling and post-buckling behaviour under axial compression. Thin-Walled Structures, 107, 335-344.

[16] Banat, D., & Mania, R. J. (2017). Failure assessment of thin-walled FML profiles during buckling and postbuckling response. Composites Part B: Engineering, 112, 278-289.

[17] Banat, D., & Mania, R. J. (2018). Progressive failure analysis of thin-walled Fibre Metal Laminate columns subjected to axial compression. Thin-Walled Structures, 122, 52-63.

[18] Dhaliwal, G. S., & Newaz, G. M. (2017). Compression after impact characteristics of carbon fiber reinforced aluminum laminates. Composite Structures, 160, 1212-1224.

[19] Lezgy-Nazargah, M. (2017). A generalized layered global-local beam theory for elasto-plastic analysis of thin-walled members. Thin-Walled Structures, 115, 48-57.

[20] Mohandes, M., & Ghasemi, A. R. (2017). Modified couple stress theory and finite strain assumption for nonlinear free vibration and bending of micro/nanolaminated composite Euler–Bernoulli beam under thermal loading. Proceedings of the Institution of Mechanical Engineers, Part C: Journal of Mechanical Engineering Science, 231(21), 4044-4056.

[21] Mohandes, M., Ghasemi, A. R., Irani-Rahagi, M., Torabi, K., & Taheri-Behrooz, F. (2018). Development of beam modal function for free vibration analysis of FML circular cylindrical shells. Journal of Vibration and Control, 24(14), 3026-3035.

[22] Ahmadi, H., & Rasheed, H. A. (2018). Lateral torsional buckling of anisotropic laminated thin-walled simply supported beams subjected to mid-span concentrated load. Composite Structures, 185, 348-361.

[23] Wackerfuß, J., & Kroker, A. M. (2018). An efficient semi-analytical simulation framework to analyse laminated prismatic thin-walled beams. Computers & Structures, 208, 32-50.

[24] Asadi, A., Sheikh, A. H., & Thomsen, O. T. (2019). Buckling behaviour of thin-walled laminated composite beams having open and closed sections subjected to axial and end moment loading. Thin-Walled Structures, 141, 85-96.

[25] Ghasemi, A. R., & Mohandes, M. (2019). Comparison between the frequencies of FML and composite cylindrical shells using beam modal function model. Journal of Computational Applied Mechanics, 50(2), 239-245.

[26] Soltani, M. (2020). Flexural-torsional stability of sandwich tapered I-beams with a functionally graded porous core. International Journal of Numerical Methods in Civil Engineering, 4(3), 8-20.

[27] Lezgy-Nazargah, M. (2014). An isogeometric approach for the analysis of composite steel–concrete beams. Thin-Walled Structures, 84, 406-415.

[28] Lezgy-Nazargah, M., & Kafi, L. (2015). Analysis of composite steel-concrete beams using a refined high-order beam theory. Steel and Composite Structures, 18(6), 1353-1368.

[29] Lezgy-Nazargah, M., Vidal, P., & Polit, O. (2019). A sinus shear deformation model for static analysis of composite steel-concrete beams and twin-girder decks including shear lag and interfacial slip effects. Thin-Walled Structures, 134, 61-70.

[30] Lezgy-Nazargah, M. (2020). A finite element model for static analysis of curved thin-walled beams based on the concept of equivalent layered composite cross section. Mechanics of Advanced Materials and Structures, 1-14.

[31] Lezgy-Nazargah, M., Vidal, P., & Polit, O. (2021). A quasi-3D finite element model for the analysis of thin-walled beams under axial–flexural–torsional loads. Thin-Walled Structures, 164, 107811.

[32] Einafshar, N., Lezgy-Nazargah, M., & Beheshti-Aval, S. B. (2021). Buckling, post-buckling and geometrically nonlinear analysis of thin-walled beams using a hypothetical layered composite cross-sectional model. Acta Mechanica, 1-18.

[33] Vlasov, V. Z. (1959). Thin-walled elastic beams. *PST Catalogue, 428*.

[34] Asgarian, B., Soltani, M., & Mohri, F. (2013). Lateral-torsional buckling of tapered thin-walled beams with arbitrary cross-sections. Thin-walled structures, 62, 96-108.

[35] Soltani, M., Asgarian, B., & Mohri, F. (2019). Improved finite element model for lateral stability analysis of axially functionally graded nonprismatic I-beams. International Journal of Structural Stability and Dynamics, 19(09), 1950108.

[36] Soltani, M., & Asgarian, B. (2020). Lateral-Torsional Stability Analysis of a Simply Supported Axially Functionally Graded Beam with a Tapered I-Section. Mechanics of Composite Materials, 1-16.

[37] Benyamina, A.B., Meftah, S.A., Mohri, F.: Analytical solutions attempt for lateral torsional buckling of doubly symmetric web-tapered I-beams. Engineering structures. **56**, 1207-1219 (2013).

[38] Raftoyiannis, I.G. & Adamakos, T. (2010). Critical lateral-torsional buckling moments of steel web-tapered I-beams. The Open Construction and Building Technology Journal, 4(1).

[39] Osmani, A., & Meftah, S. A. (2018). Lateral buckling of tapered thin walled bi-symmetric beams under combined axial and bending loads with shear deformations allowed. Engineering Structures, 165, 76-87.

[40] Soltani, M., & Sistani, A. (2017). Elastic stability of columns with variable flexural rigidity under arbitrary axial load using the finite difference method. International Journal of Numerical Methods in Civil Engineering, 1(4), 23-31.

[41] Soltani, M., Asil Gharebaghi, S., & Mohri, F. (2018). Lateral stability analysis of steel tapered thin-walled beams under various boundary conditions. International Journal of Numerical Methods in Civil Engineering, 3(1), 13-25.

[42] Soltani, M., & Mohammadi, M. (2018). Stability Analysis of Non-Local Euler-Bernoulli Beam with Exponentially Varying Cross-Section Resting on Winkler-Pasternak Foundation. International Journal of Numerical Methods in Civil Engineering, 2(3), 67-77.

[43] Soltani, M., & Gholamizadeh, A. (2018). Size-dependent buckling analysis of non-prismatic Timoshenko nanobeams made of FGMs rested on Winkler foundation. International Journal of Numerical Methods in Civil Engineering, 3(2), 35-46.

[44] Soltani, M., & Mohri, F. (2016). Stability and vibration analyses of tapered columns resting on one or two-parameter elastic foundations. International Journal of Numerical Methods in Civil Engineering, 1(2), 57-66.

[45] Soltani, M. (2017). Vibration characteristics of axially loaded tapered Timoshenko beams made of functionally

graded materials by the power series method. International Journal of Numerical Methods in Civil Engineering, 2(1), 1-14.
[46] Soltani, M. (2020). Finite element modelling for buckling analysis of tapered axially functionally graded Timoshenko beam on elastic foundation. Mechanics of Advanced Composite Structures.
[47] ANSYS, Version 5.4, Swanson Analysis System, Inc, 2007.